Mixing between flavor singlets in lattice gauge theories coupled to matter fields in multiple representations

Ed Bennett,[1,*] Niccolò Forzano,[2,†] Deog Ki Hong,[3,4,‡] Ho Hsiao,[5,§] Jong-Wan Lee,[6,‖] C.-J. David Lin,[5,7,8,¶] Biagio Lucini,[**,1,9] Maurizio Piai,[2,††] Davide Vadacchino,[10,‡‡] and Fabian Zierler[2,§§]

[1]*Swansea Academy of Advanced Computing, Swansea University (Bay Campus), Fabian Way, SA1 8EN Swansea, Wales, United Kingdom*
[2]*Department of Physics, Faculty of Science and Engineering, Swansea University, Singleton Park, SA2 8PP, Swansea, Wales, United Kingdom*
[3]*Department of Physics, Pusan National University, Busan 46241, Korea*
[4]*Extreme Physics Institute, Pusan National University, Busan 46241, Korea*
[5]*Institute of Physics, National Yang Ming Chiao Tung University, 1001 Ta-Hsueh Road, Hsinchu 30010, Taiwan*
[6]*Particle Theory and Cosmology Group, Center for Theoretical Physics of the Universe, Institute for Basic Science (IBS), Daejeon, 34126, Korea*
[7]*Centre for Theoretical and Computational Physics, National Yang Ming Chiao Tung University, 1001 Ta-Hsueh Road, Hsinchu 30010, Taiwan*
[8]*Centre for High Energy Physics, Chung-Yuan Christian University, Chung-Li 32023, Taiwan*
[9]*Department of Mathematics, Faculty of Science and Engineering, Swansea University (Bay Campus), Fabian Way, SA1 8EN Swansea, Wales, United Kingdom*
[10]*Centre for Mathematical Sciences, University of Plymouth, Plymouth, PL4 8AA, United Kingdom*

(Received 19 July 2024; accepted 10 September 2024; published 7 October 2024)

We provide the first extensive, numerical study of the nontrivial problem of mixing between flavor-singlet composite states emerging in strongly coupled lattice field theories with matter field content consisting of fermions transforming in different representations of the gauge group. The theory of interest is the minimal candidate for a composite Higgs model that also accommodates a mechanism for top partial compositeness: the $Sp(4)$ gauge theory coupled to two (Dirac) fermions transforming as the fundamental and three as the two-index antisymmetric representation of the gauge group, respectively. We apply an admixture of APE smearing and Wuppertal smearings, as well as the generalized eigenvalue problem approach, to two-point functions involving flavor-singlet mesons, for ensembles having time extent longer than the space extent. We demonstrate that, in the region of lattice parameter space accessible to this study, both masses and mixing angles can be measured effectively, despite the presence of (numerically noisy) contributions from disconnected diagrams.

DOI: 10.1103/PhysRevD.110.074504

I. INTRODUCTION

A distinguishing feature of a broad class of models of new physics featuring composite dynamics is the emergence in their spectrum of several scalar singlets, associated with spontaneously broken, approximate, anomalous Abelian continuous symmetries [1]. In the context of composite Higgs models (CHMs) [2–4] that also implement top partial compositeness (TPC) [5],[1] the multiplicity

*Contact author: E.J.Bennett@swansea.ac.uk
†Contact author: 2227764@swansea.ac.uk
‡Contact author: dkhong@pusan.ac.kr
§Contact author: thepaulxiao.sc06@nycu.edu.tw
‖Contact author: j.w.lee@ibs.re.kr
¶Contact author: dlin@nycu.edu.tw
**Contact author: B.Lucini@Swansea.ac.uk
††Contact author: m.piai@swansea.ac.uk
‡‡Contact author: davide.vadacchino@plymouth.ac.uk
§§Contact author: fabian.zierler@swansea.ac.uk

[1]An incomplete catalog of such models, in which the Higgs fields of the Standard Model emerge as pseudo-Nambu-Goldstone bosons (PNGBs) associated with the spontaneous breaking of approximate global symmetries, and of studies of their phenomenology, includes for example Refs. [6–48]. Implementations of similar ideas within gauge-gravity dualities have been presented for example in Refs. [49–56] and, more recently, in Refs. [57–63], in the bottom-up approach, and Ref. [64] in the top-down approach to holography.

of such flavor-singlet states arises because the short-distance origin of the dynamics involves two separate matter sectors coupled to the same gauge theory.[2] Examples can be found in the reviews [70–72], and the tables in Refs. [73–75]. Closely related classes of theories are also known to admit an application as new models of dark matter with strongly coupled origin, for example along the lines of Refs. [76–88].

The existence of mixing terms in the effective field theory (EFT) description of such flavor singlets is ensured by the chiral anomaly, which breaks the symmetry even when no other explicit symmetry-breaking terms are present. The phenomenology associated with such scalar singlets is determined by coefficients in the EFT treatment that have dynamical origin—related to that of axionlike particles [89–91]. This is the case in the dark matter context, as in the collider phenomenology one [1,19,75,92–94]. Hence, gaining nonperturbative information about them is essential in order to plan and perform an effective program of experimental searches for new particles in both visible and dark sectors.

In recent years, extensive numerical investigations have been developed in the context of extensions to the Standard Model, based on symplectic gauge groups $SU(2) = Sp(2)$ [95–106] and $Sp(4)$ [107–123]. Among the gauge theories with fermions in two distinct representations, lattice studies have been performed in $SU(2)$ [124,125], as well as in $Sp(4)$ gauge theories [113,121,123,126]. In a parallel development, studies of theories with fermions transforming in multiple representations of $SU(4)$ have also appeared [127–135]. These lattice studies, motivated by new physics considerations, focus predominantly on the study of flavored mesons.[3] This lattice subfield is only beginning to enter its high precision phase, after the necessary exploratory period. Calculating correlation functions involving singlet mesons requires specific technology, developed to handle effectively the contributions to observables coming from disconnected diagrams, which potentially reduce the signal-to-noise ratio. Only a few studies in the context of physics beyond the Standard Model (BSM) outside of $SU(3)$ theories exist [99,105,116]. To the best of our knowledge, this paper is the first one to present a systematic lattice study of the effects of mixing between different flavor singlets in models of BSM physics. Our aim is to demonstrate the feasibility of such an endeavor.

[2]This requirement may not apply in $SU(3)$ theories, for which the ordinary baryons may provide the origin of the TPC fields [65]—see also the constructions in Refs. [66,67], which make use of ideas from Refs. [68,69].

[3]The literature on the $SU(3)$ theory with $N_f = 8$ Dirac fermions in the fundamental representation [136–143] or $n_s = 2$ sextets [144–149], stands out as it presents extensive studies of the flavor singlet states. But these studies focus on the phenomenology of the dilaton, the Goldstone boson associated with scale invariance, which has different quantum numbers from the PNGBs associated with Abelian internal symmetries.

In this publication, we present the first results of the calculation of the mass spectrum of spin-0, flavor singlet states with negative parity, in the presence of two distinct Abelian PNGBs associated with two $U(1)$ factors. One of them is expected to be anomalously broken, thus giving an extra contribution to the mass of one PNGB [1]. The lattice ensembles we study are obtained in the CHM candidate of Ref. [12]: the $Sp(4)$ gauge theory coupled to $N_f = 2$ (Dirac) fermions transforming according to the fundamental, as well as $N_{as} = 3$ fermions transforming as the two-index antisymmetric representation of the group. We use the ensembles described in detail in Ref. [150], originally produced to study the spectral density of flavored meson correlators, within the Hansen-Lupo-Tantalo method [134,151]. Building on the results discussed in the Appendix of Ref. [116], we introduce Wuppertal [152–155] and APE smearing [156,157]. We then implement a variation of the generalized eigenvalue problem (GEVP) to take into account mixing effects between states that appear in two-point functions involving the two distinct meson singlets in the theory.

The paper is organized as follows. We very briefly introduce the continuum and lattice theories of interest in Secs. II and III, respectively. We provide the minimal amount of detail to make the narrative self-contained, and refer the reader to Ref. [150] for technical details and in-depth discussions. Nevertheless, we extensively describe the properties of the flavor-singlet meson states of interest, with particular reference to decay constants and mixing angles, as well as our analysis techniques, in Sec. III A. Our results are then reported and critically discussed in Sec. IV. A final summary in Sec. V contains also a brief outlook on future avenues for research.

II. ELEMENTS OF FIELD THEORY

We study the $Sp(4)$ gauge theory coupled to two Dirac fermions transforming in the fundamental representation and three Dirac fermions in the antisymmetric representation of the gauge group. The Lagrangian density, in Minkowski space, is given by

$$\mathcal{L} = -\frac{1}{2}\mathrm{Tr}G_{\mu\nu}G^{\mu\nu} + \sum_{I=1}^{2}\bar{Q}^I(i\gamma^\mu D_\mu - m^{\mathrm{f}})Q^I + \sum_{K=1}^{3}\bar{\Psi}^k(i\gamma^\mu D_\mu - m^{\mathrm{as}})\Psi^k, \tag{1}$$

where Q^I, with $I = 1, 2$, are the fundamental Dirac fermions and Ψ^k, with $k = 1, 2, 3$, are the antisymmetric Dirac fermions with their respective degenerate masses m^{f} and m^{as}. The field-strength tensor for the $Sp(4)$ theory is denoted as $G_{\mu\nu} \equiv G^a_{\mu\nu}T^a$, with the Hermitian generators normalized so that $\mathrm{Tr}T^aT^b = \frac{1}{2}\delta^{ab}$, for $a, b = 1, \ldots, 10$.

In the limit of vanishing fermion masses, the Lagrangian density is invariant under the enhanced global internal symmetry with group $U(1)\times U(1)\times SU(6)\times SU(4)$. This symmetry of the Lagrangian is not reflected in low-energy physics; it is broken spontaneously by the fermion condensates. The breaking pattern is governed by the realness of the antisymmetric representation and the pseudorealness of the fundamental representation; $SU(6)$ breaks to its $SO(6)$ subgroup, while $SU(4)$ breaks to $Sp(4)$ [158]. At the same time, the diagonal and degenerate mass terms induce explicit symmetry breaking, according to the same, aligned symmetry breaking pattern. For small fermion masses, the spontaneous breaking leads to 20 PNGBs in the antisymmetric sector and 5 PNGBs in the fundamental sector [159]. In the CHM context, one can choose appropriate embeddings for the standard-model gauge group so that part of the global symmetry is (weakly) gauged. For example, in this way the five PNGBs of the fundamental sector can be identified with the Higgs doublet and one additional singlet [12]. In this paper we consider the $Sp(4)$ gauge theory in complete isolation, ignoring the effects due to coupling to other external sectors.

In theories with only one species of fermions, the global U(1) is anomalous, and no Goldstone bosons, related to its breaking, appear. In the large-N limit, the associated pseudoscalar flavor-singlet, η', becomes the would-be Goldstone mode, as the effects of the axial anomaly are suppressed in this limit [160–162]. In the presence of fermions in two distinct representations, the axial anomaly can only break one (linear combination) of the two global $U(1)$ symmetry factors. Hence, an additional PNGB is expected to appear at small fermion masses, in the pseudoscalar flavor-singlet sector, the lightest mass eigenstate in this channel. The other pseudoscalar flavor singlet should acquire a larger mass through the axial anomaly and show up as an excited state in the same channel [93].

In this paper, we perform the first measurement of flavor-singlet ground and excited states in a theory with multiple fermion representations, which we call η'_l and η'_h.[4] The theory of interest has $Sp(4)$ gauge group, and explicit mass terms for the fermions, which are not small. Hence, we expect both the aforementioned flavor singlets to be comparatively heavy, as the mass terms contribute together with the anomaly to the explicit symmetry breaking. One can draw an analogy between this regime and the $\eta-\eta'$ system in the theory of strong nuclear interactions, QCD.[5] In this case, the η meson is a PNGB accommodated within the approximate $SU(3)$ flavor symmetry, while the η' is the would-be-PNGB associated with the anomalously broken global $U(1)$. Within QCD, both the mass spectrum and the mixing between those states have been studied in detail [163–173].

[4]Note, that this corresponds to the states a and η' in the notation of Ref. [1].

[5]Note, that this analogy has its limits. In QCD, the mixing between the η and the η' is introduced by an explicit breaking of the global flavor symmetry. For the mixed representations system, this is not the case, and both states are pseudoscalar singlets even without additional symmetry breaking.

III. NUMERICAL STRATEGY

Our numerical analysis is based on ensembles generated using the Wilson plaquette action for the gauge sector and standard Wilson fermions for both the fundamental and antisymmetric fermions [174]. We consider hypercubic lattices with a volume $L^3\times T=a^4(N_s^3\times N_t)$, where a is the lattice spacing. The ensembles have been generated using the Grid software library [175–177] which has been extended to $Sp(2N)$ gauge theories [117]. We study five ensembles, at three different values of the bare fundamental fermion mass, $am_0^{\mathrm{f}}=-0.7,-0.71,0.72$, while we keep the antisymmetric fermion mass fixed, $am_0^{\mathrm{as}}=-1.01$. We consider only one value of the inverse gauge coupling, $\beta=8/g^2=6.5$. The measurements of the mesonic correlation function are performed using the HiRep code [178–180]. The configurations have been converted to the HiRep binary format using the GLU library [181]. We set the overall scale using the Wilson flow [182], the lattice implementation of the gradient flow [183,184], by calculating the gradient flow quantity, w_0 [185], in units of the lattice spacing, a. For further information on the generation of these ensembles we refer to Ref. [150]. Detailed characterization of the five ensembles is summarized in Table I.

We determine the ground state energy as well as the energy of the first excited state for the system of interest by using a variational analysis [186,187]. To this purpose, we measure the (zero-momentum) correlation matrix for a set of interpolating operators, $\{O_i\}$, which can be expanded in the Hamiltonian eigenstates as

$$C_{ij}(t-t')=\langle\bar{O}_i(t)O_j(t')\rangle=\sum_n\frac{1}{2E_n}\langle 0|\bar{O}_i|n\rangle\langle n|O_j|0\rangle e^{-E_n(t-t')}. \quad (2)$$

The eigenvalues of C_{ij} are obtained by solving the GEVP with eigenvalues $\lambda_n(t,t_0)$ and eigenvectors $v_n(t,t_0)$ given by

$$C(t)v_n(t,t_0)=\lambda_n(t,t_0)C(t_0)v_n(t,t_0). \quad (3)$$

Assuming that the states created by each of the operators in the variational basis have a sufficient overlap with the first M eigenstates in the selected channel, the leading behavior of the mth eigenvalue at large t for fixed but sufficiently large t_0 can be written as [188]

TABLE I. Ensembles studied in this paper. For each of the five ensembles, we list the value of the inverse lattice coupling, β, the masses of the two fermion species, am_0^{as} and am_0^{f}, the extent of the lattice in time, N_t, and space directions, N_s, the number of thermalization steps, N_{therm}, discarded from the analysis, the number of complete sweeps, n_{skip}, discarded between configurations retained in the analysis, the number of configurations constituting the ensemble and used in the analysis, N_{conf}, the average plaquette in the ensemble, $\langle P\rangle$, the value of the Wilson flow scale, w_0/a, the topological autocorrelation time in configuration units, τ_{int}^{Q}, and the average topological charge in the ensemble, $\bar{Q}$. Details, explanations and discussions can be found in Ref. [150].

Label	β	am_0^{as}	am_0^{f}	N_t	N_s	N_{therm}	n_{skip}	N_{conf}	$\langle P\rangle$	w_0/a	τ_{int}^{Q}	$\bar{Q}$
M1	6.5	−1.01	−0.71	48	20	3006	14	479	0.585172(16)	2.5200(50)	6.9(2.4)	0.38(12)
M2	6.5	−1.01	−0.71	64	20	1000	28	698	0.585172(12)	2.5300(40)	7.1(2.1)	0.58(14)
M3	6.5	−1.01	−0.71	96	20	4000	26	436	0.585156(13)	2.5170(40)	6.4(3.3)	−0.60(19)
M4	6.5	−1.01	−0.70	64	20	1000	20	709	0.584228(12)	2.3557(31)	10.6(4.8)	−0.31(19)
M5	6.5	−1.01	−0.72	64	32	3020	20	295	0.5860810(93)	2.6927(31)	12.9(8.2)	0.80(33)

$$\lambda_m(t\to\infty,t_0)=e^{-E_m(t-t_0)}+\mathcal{O}(e^{-(E_{m+1}-E_m)t}). \quad (4)$$

In summary, the solution of the above GEVP enables us to find the operator that produces states with the maximal overlap with the ground state and the first excited state, and thus to access their energies.

The two meson operators of interest in the pseudoscalar singlet channel are coupled, respectively, to N_{f} fundamental fermions and N_{as} antisymmetric fermions, and they are given by the following[6]:

$$O_{\eta^{\mathrm{as}}}(x)=\frac{1}{\sqrt{N_{\mathrm{as}}}}\sum_{k=1}^{N_{\mathrm{as}}}\bar{\Psi}^k(x)\gamma_5\Psi^k(x), \quad (5)$$

$$O_{\eta^{\mathrm{f}}}(x)=\frac{1}{\sqrt{N_{\mathrm{f}}}}\sum_{I=1}^{N_{\mathrm{f}}}\bar{Q}^I(x)\gamma_5 Q^I(x). \quad (6)$$

Performing the required Wick contractions for the correlation matrix resulting from Eq. (2), for operators at lattice sites x and y, we find the diagrammatic expression

$$C_{11}(x,y)\equiv\langle\bar{O}_{\eta^{\mathrm{as}}}(x)O_{\eta^{\mathrm{as}}}(y)\rangle=-$$

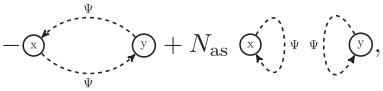

$$+N_{\mathrm{as}}$$

$$, \quad (7)$$

$$C_{22}(x,y)\equiv\langle\bar{O}_{\eta^{\mathrm{f}}}(x)O_{\eta^{\mathrm{f}}}(y)\rangle=-$$

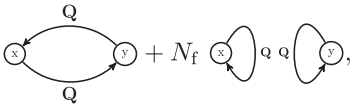

$$+N_{\mathrm{f}}$$

$$, \quad (8)$$

$$C_{12}(x,y)=C_{21}(x,y)\equiv\langle\bar{O}_{\eta^{\mathrm{f}}}(x)O_{\eta^{\mathrm{as}}}(y)\rangle=+\sqrt{N_{\mathrm{as}}N_{\mathrm{f}}}$$

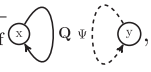

$$, \quad (9)$$

where dashed lines denote the contraction of two antisymmetric fermion fields and solid lines denote the contraction of two fundamental fermion fields. Unlike the singlet-octet basis in QCD for the η and η' mesons, the cross-correlator does not vanish in the limit of vanishing fermion masses; hence we expect sizeable mixing effects for moderate and light fermion masses.

The disconnected diagrams in Eqs. (7)–(9) are challenging for lattice calculations, as they introduce a smaller signal-to-noise ratio than the connected diagrams—that are also present in nonsinglet mesons. Our objective is to improve the signal by enlarging the variational basis through smearing techniques. The general principle at work is that one expects the adoption of a larger variational

[6]We note, that in principle a contribution from the $J^P=0^-$ glueball state is also allowed. However, an investigation of η'-glueball mixing in two-flavor QCD showed no sizeable contributions from the glueball state [189]. Studies of the quenched $Sp(4)$ theory suggest that indeed the 0^- glueballs is very heavy with respect to the scale of the vector mesons—see Fig. 13 of Ref. [121], for example.

basis in the GEVP analysis to suppress the effects of excited state contamination at smaller Euclidean times, where the signal-to-noise ratio is substantially better.

We implement Wuppertal smearing of the fermionic operators [152–155], in conjunction with APE smearing for the gauge fields [156,157]. We follow the approach used in Ref. [121] for the connected diagrams, and apply the smearing function to point sources. For the disconnected diagrams, we use spin-diluted stochastic sources [190], with $Z_2 \times Z_2$ noise [191], and perform the measurements on $n_{\rm src} = 64$ stochastic samples. As pointed out in Ref. [170], it is possible to measure the disconnected loops at several smearing levels using only one inversion of the Dirac operator. Doing so comes at the cost of potentially introducing a bias in the construction of the full correlation function, following the procedure deployed in Ref. [99]. The construction of a completely unbiased estimator would require one to perform a separate inversion for every smearing level, but this would go beyond the purposes of this paper. We apply APE smearing for every measurement. We choose the smearing parameter as $\alpha_{\rm APE} = 0.4$, with $N_{\rm APE} = 50$ smearing steps.

The variational basis is composed of the operators defined in Eqs. (5) and (6) together with their Wuppertal-smeared versions, with $N^{\rm smear} = 10, 20, \ldots, 80$ smearing steps, and $\epsilon_{\rm f} = 0.2$ for the fundamental fermions, or $\epsilon_{\rm as} = 0.12$ for the antisymmetric fermions (we follow the notation of Ref. [121], to which we refer the reader for technical details). In total, we have a variational basis of 18 operators.

For a finite sample, the correlation functions of pseudoscalar flavor-singlet mesons (or any other quantity that has the same quantum numbers as the topological charge density) can acquire an additional, constant contribution [192]. In order to remove this constant we consider the central difference approximation to the derivative of the correlation matrix, as proposed in Ref. [193] and use of the following redefinition:

$$C_{ij}(t) \to \tilde{C}_{ij}(t) = \frac{C_{ij}(t-1) - C_{ij}(t+1)}{2}. \quad (10)$$

Doing so changes the periodicity of the correlation matrix with respect to the lattice midpoint, $t = T/2$, from periodic to antiperiodic [116].

After performing the GEVP analysis, we fit the eigenvalues to an exponentially decaying function according to Eq. (4). We first visually examine the effective mass, $m_{\rm eff}(t)$, defined implicitly as

$$\frac{\lambda(t-1)}{\lambda(t)} = \frac{e^{-m_{\rm eff}(t)\cdot(T-t+1)} \pm e^{-m_{\rm eff}(t)\cdot(t-1)}}{e^{-m_{\rm eff}(t)\cdot(T-t)} \pm e^{-m_{\rm eff}(t)\cdot t}}. \quad (11)$$

We solve for the effective mass numerically using a root finding algorithm. It exhibits a plateau when the eigenvalue is dominated by its leading exponential term at large Euclidean time. The sign in Eq. (11) is chosen to be positive for symmetric correlation functions, and negative for antisymmetric ones. We then perform a fit to the eigenvalue using constrained curve fitting [194], utilizing the CORRFITTER package [195].

Finally, in order to gauge the physical meaning of the results of our analysis, we use the same ensembles and processes also to perform the measurement of the mass of the lightest flavored mesons, in the pseudoscalar and vector channel, for mesons constructed with either species of fermions. We denote as PS(ps) flavored pseudoscalar mesons made of vfermions transforming in the fundamental, f, (antisymmetric, as) representation, and as V(v) flavored vector mesons with the same composition. We refer the reader to Ref. [150] for more details about the operators, and the spectrum of flavored mesons, that are not central to the results and discussions presented in this paper.

A. Decay constants and mixing angles

It is interesting to extract the mixing angle between the lightest states sourced by the operators in Eqs. (5) and (6). For the purposes of this paper, we assume that the state mixing is given by the mixing of the decay constants. We call η'_l and η'_h, respectively, the lightest and next-to-lightest states identified in the GEVP analysis. We parametrize the nonrenormalized matrix elements of axial-vector currents with the pseudoscalar singlets as follows:

$$\begin{pmatrix} F_{\rm f}^{\eta'_l} p_\mu^{\eta'_l} & F_{\rm as}^{\eta'_l} p_\mu^{\eta'_l} \\ F_{\rm f}^{\eta'_h} p_\mu^{\eta'_h} & F_{\rm as}^{\eta'_h} p_\mu^{\eta'_h} \end{pmatrix} \equiv \begin{pmatrix} \langle 0| \frac{1}{\sqrt{N_{\rm f}}} \sum_{i=1}^{N_{\rm f}} \bar{Q}_i(x)\gamma_\mu\gamma_5 Q_i(x)|\eta'_l\rangle & \langle 0| \frac{1}{\sqrt{N_{\rm as}}} \sum_{i=1}^{N_{\rm as}} \bar{\Psi}_i(x)\gamma_\mu\gamma_5 \Psi_i(x)|\eta'_l\rangle \\ \langle 0| \frac{1}{\sqrt{N_{\rm f}}} \sum_{i=1}^{N_{\rm f}} \bar{Q}_i(x)\gamma_\mu\gamma_5 Q_i(x)|\eta'_h\rangle & \langle 0| \frac{1}{\sqrt{N_{\rm as}}} \sum_{i=1}^{N_{\rm as}} \bar{\Psi}_i(x)\gamma_\mu\gamma_5 \Psi_i(x)|\eta'_h\rangle \end{pmatrix}. \quad (12)$$

In this general relation, we define the relevant decay constants computed with an operator (op) and a state (s) as F^s_{op}. By setting $\mu = 0$ we obtain the familiar relation

$$\begin{pmatrix} F_{\rm f}^{\eta'_l} p_0^{\eta'_l} & F_{\rm as}^{\eta'_l} p_0^{\eta'_l} \\ F_{\rm f}^{\eta'_h} p_0^{\eta'_h} & F_{\rm as}^{\eta'_h} p_0^{\eta'_h} \end{pmatrix} = \begin{pmatrix} F_{\rm f}^{\eta'_l} m_{\eta'_l} & F_{\rm as}^{\eta'_l} m_{\eta'_l} \\ F_{\rm f}^{\eta'_h} m_{\eta'_h} & F_{\rm as}^{\eta'_h} m_{\eta'_h} \end{pmatrix}. \quad (13)$$

These nonrenormalized local matrix elements can be obtained from the eigenvectors of the GEVP analysis, for a variational basis without Wuppertal smearing. This matrix is parametrized as follows, in terms of two mixing angles, and two decay constants [196]:

$$\begin{pmatrix} F_{\mathrm{f}}^{\eta_l'} & F_{\mathrm{as}}^{\eta_l'} \\ F_{\mathrm{f}}^{\eta_h'} & F_{\mathrm{as}}^{\eta_h'} \end{pmatrix} \equiv \begin{pmatrix} F_{\eta_l'}\cos\phi_{\eta_l'} & F_{\eta_l'}\sin\phi_{\eta_l'} \\ -F_{\eta_h'}\sin\phi_{\eta_h'} & F_{\eta_h'}\cos\phi_{\eta_h'} \end{pmatrix}, \tag{14}$$

in analogy to the $\eta - \eta'$ mixing system in the singlet-octet basis of QCD.

For this work, we choose a variational basis of interpolating operators and the matrix elements of the currents according to Eqs. (5), (6), and (12). The difference in mass between mesons made of antisymmetric and fundamental fermions is expected to be large for the ensembles studied in this paper, on the basis of existing numerical results for other parts of the spectrum [113]. In QCD, the two mixing angles are approximately equal, $\phi_{\eta_l'} \approx \phi_{\eta_h'}$, at the physical point [197], and Eq. (14) is effectively described by a single mixing angle, $\phi \equiv \phi_{\eta_l'} = \phi_{\eta_h'}$. We test this assumption for the present theory in Sec. IV B.

A variation of this approach requires one to use the pseudoscalar matrix elements. This alternative approach has also been successfully applied to studying $\eta - \eta'$ mixing in QCD [163–166]. Again, the matrix elements are generically parametrized in terms of two mixing angles:

$$\begin{aligned} &\begin{pmatrix} \langle 0|O_{\eta^{\mathrm{f}}}|\eta_l'\rangle & \langle 0|O_{\eta^{\mathrm{as}}}|\eta_l'\rangle \\ \langle 0|O_{\eta^{\mathrm{f}}}|\eta_h'\rangle & \langle 0|O_{\eta^{\mathrm{as}}}|\eta_h'\rangle \end{pmatrix} \\ &= \begin{pmatrix} A_{\mathrm{f}}^{\eta_l'} & A_{\mathrm{as}}^{\eta_l'} \\ A_{\mathrm{f}}^{\eta_h'} & A_{\mathrm{as}}^{\eta_h'} \end{pmatrix} \equiv \begin{pmatrix} A_{\eta_l'}\cos\phi_{\eta_l'} & A_{\eta_l'}\sin\phi_{\eta_l'} \\ -A_{\eta_h'}\sin\phi_{\eta_h'} & A_{\eta_h'}\cos\phi_{\eta_h'} \end{pmatrix}. \end{aligned} \tag{15}$$

We can extract the matrix elements of interest from the eigenvectors that diagonalize the 2×2 matrix of correlation functions defined by the local operators (i.e., without smearing). Under the assumption that only two states contribute to the 2×2 correlation matrix, the eigenvectors, $v_n(t, t_0)$, obtained from the GEVP analysis should be proportional to time-independent vectors, u_n [188]. We use this to determine the matrix elements $F_{op}^s m_s$ and A_{op}^s, by fitting the *effective mixing angle* ϕ defined as

$$-(\tan\phi)^2 \equiv \frac{A_{\mathrm{as}}^{\eta_l'} A_{\mathrm{f}}^{\eta_h'}}{A_{\mathrm{as}}^{\eta_h'} A_{\mathrm{f}}^{\eta_l'}}, \tag{16}$$

to a constant value, for a suitable interval $t \in [t_{\mathrm{min}}, t_{\mathrm{max}}]$, with $t_{\mathrm{min}} > t_0$. We further determine $\phi_{\eta_l'}$ and $\phi_{\eta_h'}$ independently to test the deviations from ϕ in a two-angle parametrization.

IV. RESULTS

We present in this section our main numerical results. First, we explain our strategy in applying the GEVP analysis. As discussed in the previous section, we applied APE smearing to the ensembles, as well as Wuppertal smearing to the meson operators. A basis of 18 distinct operators was obtained by varying the number of smearing levels applied to the operators in Eqs. (5) and (6). While the inclusion of further smearing levels in the GEVP improves the determination of the effective mass, it soon reintroduces a signal-to-noise ratio in the form of a loss signal at intermediate values of t. Hence, we identify by inspection a subset of smearing levels appropriate to our analysis. By inspection, we find that the optimal choice for our purpose is to include only a subset of the operators produced with different N^{smear}. We find that restricting ourselves to three smearing levels $N^{\mathrm{smear}} = 0, 40, 80$ is a good choice for our ensembles in all channels studied here. We observed that the stability of the GEVP analysis is improved by using a small value of $t_0 = 1$. This choice may in principle give rise to unaccounted systematic effects, that scale with $\mathcal{O}(e^{-\Delta E t_0})$, where ΔE is the energy difference to the next state that is not properly captured by the chosen variational basis [188]. In the Appendix we show that no significant deviations are observed when choosing a larger value of t_0.

A. Meson masses

In Fig. 1, we show the effective masses of the states, $am_{\eta_l'}^{\mathrm{eff}} < am_{\eta_h'}^{\mathrm{eff}}$, expressed in units of the lattice scale, a. The effective mass plots, obtained from the GEVP analysis, are shown to provide visual guidance in the choice of the fitting range. In some cases, only an approximate plateau appears within the statistical errors. This could be attributed to an insufficient stochastic sampling of the Dirac propagator. In this work we have chosen $n_{\mathrm{src}} = 64$ stochastic sources to sample the disconnected diagrams in (7)–(9). This choice introduces an error in the correlation matrix, that is expected to scale as $\mathcal{O}(1/\sqrt{n_{\mathrm{src}}})$ [198].

As can be seen in Fig. 1, the signal in the effective mass is lost for times t much smaller than the temporal lattice midpoint $T/2$. Thus, we only fit a single exponential in the specified fit interval. The choices we made for the fitting parameters and the associated $\chi^2/N_{\mathrm{d.o.f.}}$ values are reported in Table II. The extracted meson masses (expressed in lattice units) are reported in Table III. We find that the statistical uncertainties obtained for the flavor-singlet states are up to 1 order of magnitude larger than those for the flavored states. For the aforementioned reasons, it is likely that the systematic errors are also larger than those of the flavored mesons.

In Fig. 2, we show all the low-lying pseudoscalar and vector meson masses. They are displayed as a function of N_t in the left-hand panel and as a function of am_0^{f} in the

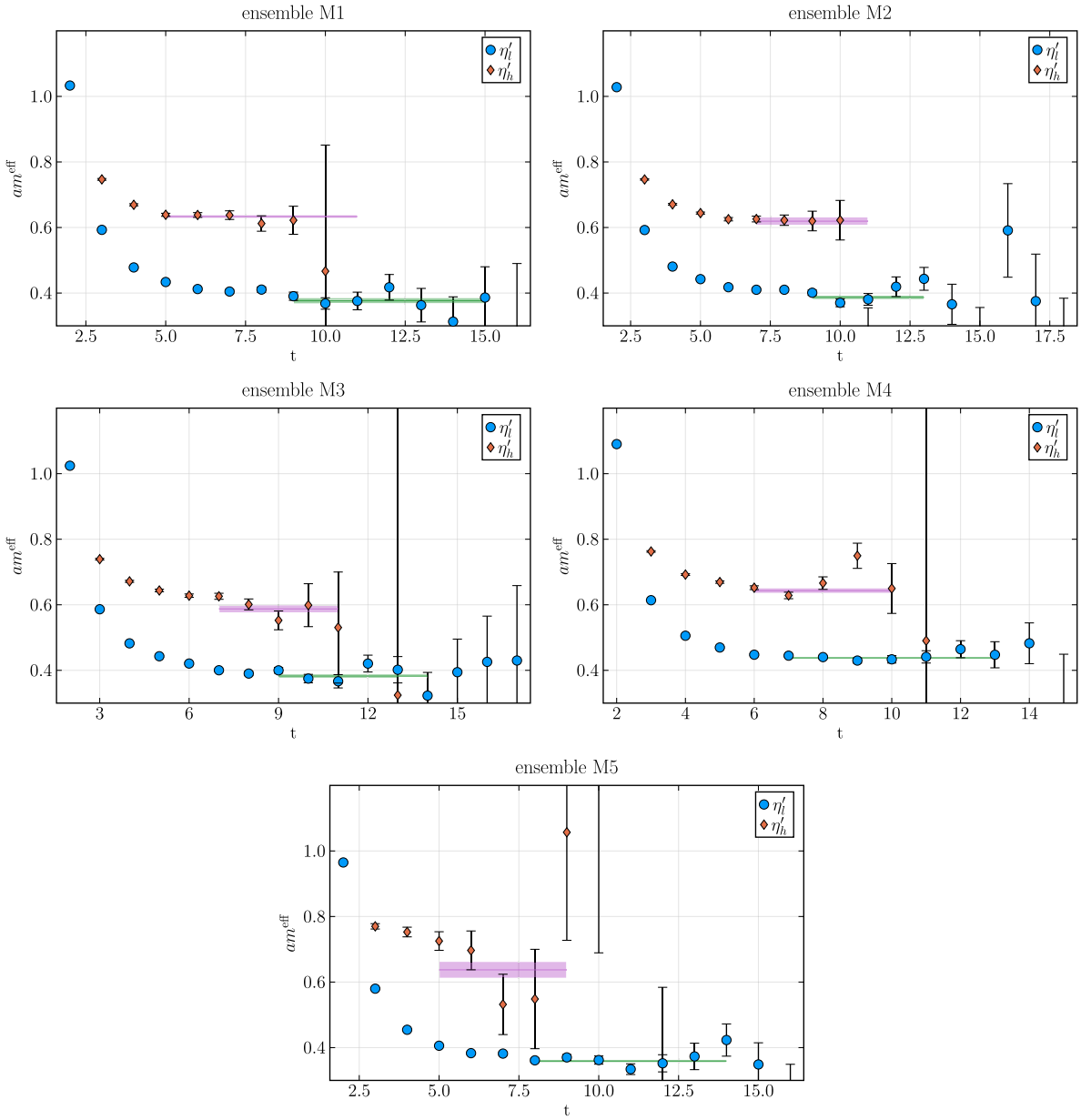

FIG. 1. Effective masses, $am^{\rm eff}_{\eta'_l} < am^{\rm eff}_{\eta'_h}$ in units of the lattice spacing, of the ground state and first excited state in the flavor singlet, pseudoscalar meson sector of the $Sp(4)$ theory coupled to two Dirac fermions transforming in the fundamental representation, f, and three in the antisymmetric, as. The effective mass makes use of the eigenvalues extracted in the GEVP analysis. We display, for comparison, also the masses as extracted by an exponential fit to the eigenvalues as colored bands. The variational analysis used three distinct levels of smearing. For some ensembles, there is no clear plateau for the first excited state. The five panels correspond to the five available ensembles.

TABLE II. Fit parameters used in the extraction of the meson masses, reported in Table III. We report the fitting ranges, I, the number of exponential terms, $N_{\rm exp}$, used in the fit, and the values of $\chi^2/N_{\rm d.o.f.}$ for every fit.

Label	$I_{\eta'_l}$	$I_{\eta'_h}$	$I_{\rm PS}$	$I_{\rm ps}$	$I_{\rm V}$	$I_{\rm v}$	$N_{\rm exp}$	$\chi^2/N_{\rm d.o.f.}$ η'_l	$\chi^2/N_{\rm d.o.f.}$ η'_h	$\chi^2/N_{\rm d.o.f.}$ PS	$\chi^2/N_{\rm d.o.f.}$ ps	$\chi^2/N_{\rm d.o.f.}$ V	$\chi^2/N_{\rm d.o.f.}$ v
M1	(9,15)	(5,11)	(7,14)	(9,14)	(7,11)	(7,14)	1	2.7	2.4	3.8	2.9	0.9	1.5
M2	(9,13)	(7,11)	(8,13)	(8,15)	(8,13)	(8,16)	1	1.8	1.9	2.7	1.7	2.3	1.8
M3	(9,14)	(7,11)	(9,16)	(10,13)	(11,20)	(10,13)	1	1.4	1.4	1.1	1.9	1.3	1.8
M4	(7,13)	(6,10)	(8,18)	(7,16)	(8,16)	(7,13)	1	2.2	2.0	1.3	2.0	1.3	3.4
M5	(8,14)	(5,9)	(9,16)	(7,13)	(12,16)	(8,13)	1	1.4	1.6	1.4	2.2	1.5	1.9

TABLE III. Meson masses extracted from large Euclidean-time behavior of the eigenvalues, $\lambda(t)$, within the GEVP analysis. We report the ground states and first excited states in the flavor-singlet pseudoscalar channel as well as the ground states for flavored pseudoscalar and vector mesons made of either species of fermions, and for all five ensembles, which we characterize by the lattice coupling, β, its number of sites in the temporal, N_t, and spatial, N_s, directions, and the bare masses of the fermions in lattice units, am_0^{f} and am_0^{as}.

Label	β	N_t	N_l	am_0^{f}	am_0^{as}	$am_{\eta_l'}$	$am_{\eta_h'}$	am_{PS}	am_{ps}	am_{V}	am_{v}
M1	6.5	48	20	−0.71	−1.01	0.3769(96)	0.6334(59)	0.3639(14)	0.6001(11)	0.4030(33)	0.6452(18)
M2	6.5	64	20	−0.71	−1.01	0.3867(68)	0.619(13)	0.3648(13)	0.59856(82)	0.4038(17)	0.6421(15)
M3	6.5	96	20	−0.71	−1.01	0.3826(67)	0.588(12)	0.3652(16)	0.59940(79)	0.4040(18)	0.6467(21)
M4	6.5	64	20	−0.7	−1.01	0.4381(33)	0.6433(88)	0.4067(13)	0.62426(85)	0.4476(17)	0.6742(13)
M5	6.5	64	32	−0.72	−1.01	0.3591(53)	0.637(26)	0.31076(68)	0.57718(85)	0.3518(12)	0.6223(15)

right-hand panel. On the same plots, we display the masses of the corresponding states in the flavored channels. Overall, the ground states and first excited state masses in the flavor-singlet channels are found to lie, within uncertainties, in the mass range of the flavored states. We find larger uncertainties for the η' state; hence the mass hierarchy is not fully determined. For the lightest ensemble, M5, the flavor-singlet pseudoscalar states have mass compatible to the flavored vector mesons.

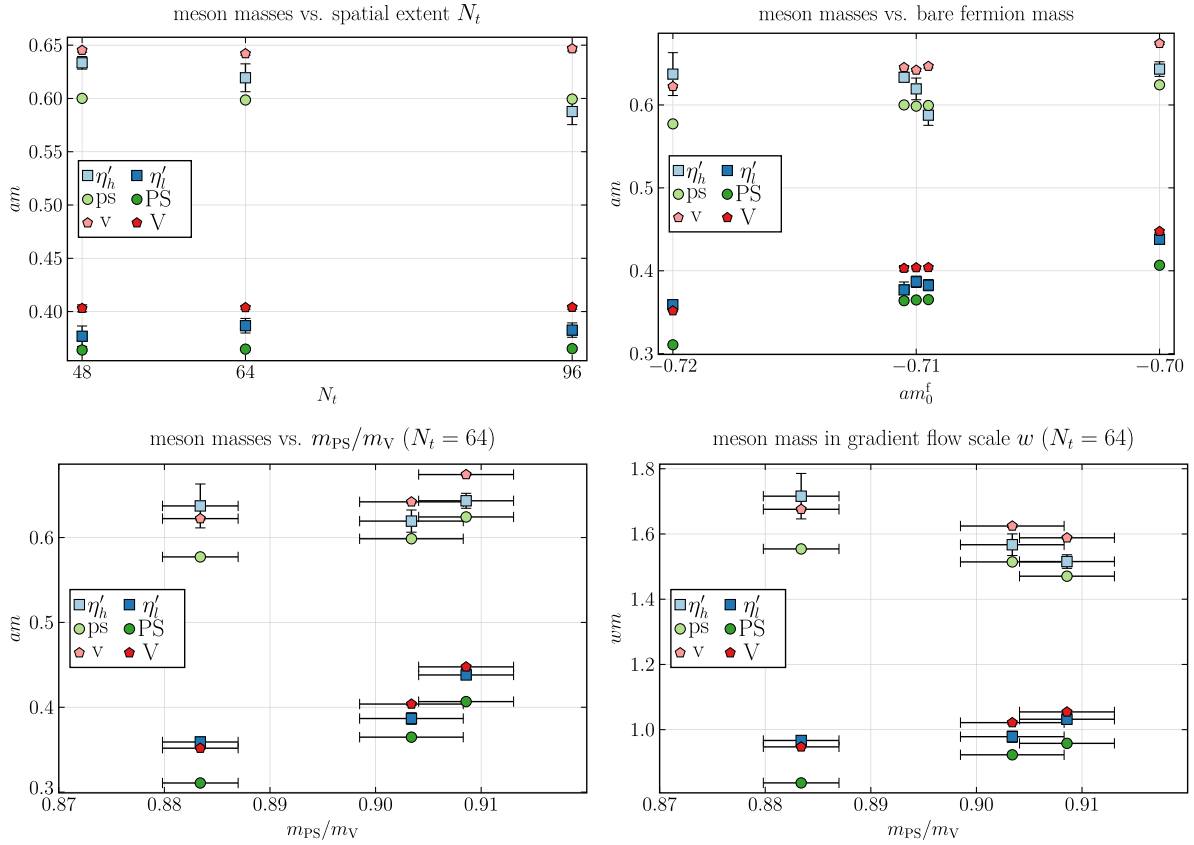

FIG. 2. Masses, am, of the lightest flavor-singlet and flavored pseudoscalar mesons, and flavored vector mesons, constituted of either species of fermions. Top left panel: measurements of the masses in lattice units for the three ensembles (M1–M3) that have common values of $am_0^{\mathrm{as}} = -1.01$ and $am_0^{\mathrm{f}} = 0.71$. The masses as shown for the three available choices of spatial lattice extent N_t. Top right panel: measurements of the masses in lattice units for the three available choices of bare fundamental fermion mass. A small horizontal offset has been introduced, for visual clarity, in the ensembles M1–M3. Bottom left panel: measurement of the masses in lattice units for all ensembles with $N_t = 64$ (M2, M4, and M5), plotted against the ratio of the mass of the flavored pseudoscalar and vector mesons constituted of fermions in the fundamental representation. Bottom right panel: same as bottom left, but the masses of the mesons are expressed in gradient flow units.

The general trends exhibited by our results suggest that the effect of the disconnected diagrams is suppressed by the heavy fermion masses present in these ensembles. Thus, the spectrum resembles that of $N_f = 2$ single-representation theories at moderately heavy to heavy fermion mass [116]. A suppression of the disconnected diagrams also implies a suppression of the $\eta'_l - \eta'_h$ mixing effects, according to Eq. (9). Thus, we expect that the associated mixing angle is small and that the state a is mostly dominated by the fundamental fermionic contribution, whereas the mass of the η' is mostly determined by the antisymmetric fermion masses. We will return to the determination of the mixing angle in the next subsection.

Because the ensembles M1–M3 share the same lattice parameters, with only the temporal lattice extent, N_t, distinguishing them, we can compare across the three to ascertain the contribution of N_t to systematic effects. We find that for both the singlet ground states, η'_l, and the first excited state, η'_h, measurements with different N_t yield compatible results. This may not be the case for further excited states [150], but these considerations go beyond the purposes of the present study.

B. Mixing angle

With the available ensembles we measured the pseudoscalar matrix elements of Eq. (15), from which we extracted the effective mixing angle, ϕ, determined according to Eq. (16), which we display in Fig. 3 as a function of the time t. A similar analysis for the axial-vector currents, in Eq. (12), did not yield a significant signal; hence we did not determine the pseudoscalar decay constants. This behavior is similar to what has been found in QCD, where the flavor-singlet axial-vector matrix elements are affected by poor signal-to-noise ratios [169].

We stress that the result for the effective mixing angle displayed in Fig. 3 have been obtained with a simplified analysis that only involves local sources. The simpler GEVP is analyzed with a larger value of $t_0 = 5$, as it is in this regime where the systematic error on the determination of the matrix element should be smaller; see Ref. [188]. We leave to future, high-precision studies the task of measuring the relevant components of the correlation matrix itself [170] to determine simultaneously the mixing angle and the decay constants.

We extract the mixing angle, ϕ, via a constant fit to the effective mixing angle. We similarly determine $\phi_{\eta'_l}$ and $\phi_{\eta'_h}$. We choose the fitting interval to start at $t = t_0 + 1$ and end at the first $t = t_{\max}$ for which the relative uncertainty in the effective mass of the flavor-singlet pseudoscalar ground state exceeds 50%. We report the extracted mixing angles in Table IV. We find a small mixing angle in all available ensembles. We find that a parametrization using two mixing angles leads to statistically significant deviations. We do not find clear evidence of mass dependence in the mixing angles ϕ and $\phi_{\eta'_l}$ in the ensembles studied here. All measurements indicate a mixing angle of roughly 6° for ϕ. These results further support earlier conclusions: because of the large value of the fermion masses, the mixing effects between the flavor-singlet pseudoscalar states η'_l and η'_h are strongly suppressed.

V. SUMMARY AND OUTLOOK

In this paper, we have presented the first numerical lattice study of the mass spectrum of flavor-singlet pseudoscalar bound states in an $Sp(4)$ gauge theory with fermions in multiple representations. The channels of interest result from the mixing effects between the Abelian PNGBs associated with the two global $U(1)$ factors in the approximate symmetry of the system. These Abelian symmetries are broken explicitly both by the masses of the fermions, and by the axial anomaly. The motivation for this study is that, in the context of composite Higgs models, the phenomenology of such flavor singlets deserves special consideration [1], and requires detailed knowledge of nonperturbative properties of the theory in its strongly coupled regime.

Our measurements have been performed on five available ensembles, generated in a lattice field theory that is of interest in its own terms, as it has been proposed as a short-distance completion to the minimal CHM that also implements top partial compositeness [12].

This type of spectroscopy measurement is challenging because it requires performing explicit calculations of disconnected diagrams contributing to the two-point functions of interest, which introduce high noise level in the numerical analysis. These measurements were obtained with a combination of APE and Wuppertal smearing, as well as with an implementation of the GEVP analysis.

The results presented above provide the first determination—and a demonstration of feasibility—of the masses of the ground and first excited state in the flavor-singlet pseudoscalar channel of this theory, as well as of their associated mixing angle.

Some limitations of the analysis descend from the fact that all the ensembles have the same value of the lattice coupling, β, so that a continuum-limit extrapolation is beyond the reach of this analysis. Furthermore, the masses for the two species of fermions belong to a regime in which the theory is far from the massless limit. As a result, the masses of neither the flavor-singlet nor the flavored pseudoscalar states in the theory are particularly light, and a massless extrapolation of the results is also beyond current reach.

The natural next step for future studies would be to deploy the numerical strategy we developed and tested in a large-scale investigation that would allow for performing continuum and massless extrapolations. This endeavor

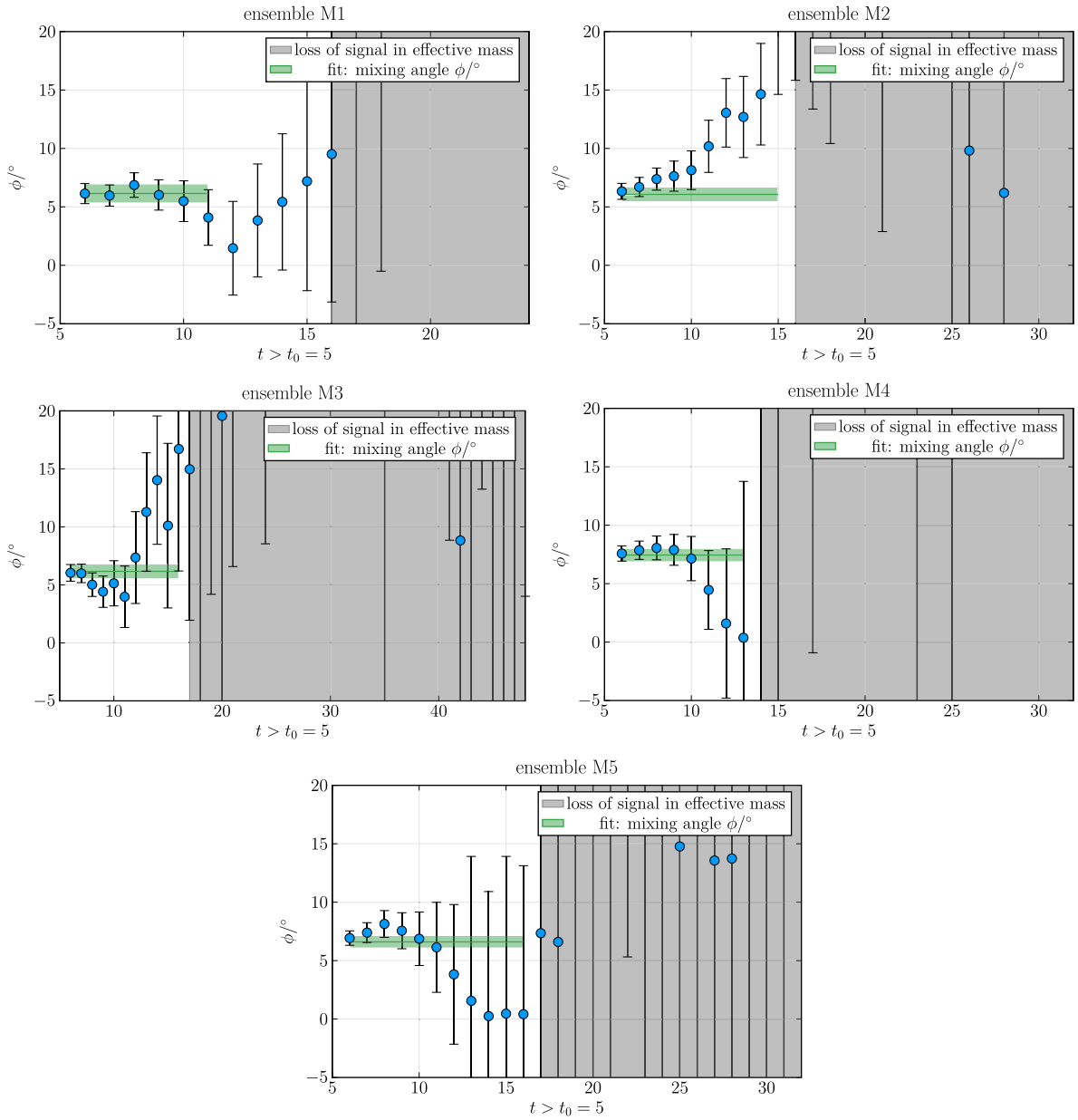

FIG. 3. Effective mixing angles, ϕ, between the lightest pseudoscalar singlets, for all ensembles M1–M5, based on the pseudoscalar singlet matrix elements defined in Eq. (15). We fit the effective mixing angle in the range from a minimum value $t = t_0 + 1$ to a maximum value $t = t_{\max}$. Conventionally, we choose the latter to coincide with the smallest t value at which the relative error of the ground-state effective mass is larger than 50%. We find good signal-to-noise ratios in all ensembles, even for the comparatively large value of $t_0 = 5$. We find no clear evidence of mass dependence of the mixing angle.

TABLE IV. Results for the pseudoscalar singlet mixing angle, ϕ, expressed in degrees, extracted from the flavor-singlet pseudoscalar matrix elements, using correlation functions with pointlike source and sink (no Wuppertal smearing). The quoted uncertainties have been obtained using jackknife resampling.

Label	β	N_t	N_s	$\phi/^\circ$	$\phi_{\eta_l'}/^\circ$	$\phi_{\eta_h'}/^\circ$
M1	6.5	48	20	6.15(83)	3.83(57)	9.8(1.1)
M2	6.5	64	20	6.07(63)	3.74(43)	9.78(89)
M3	6.5	96	20	6.16(66)	3.76(44)	10.00(92)
M4	6.5	64	20	7.44(58)	4.77(42)	12.26(86)
M5	6.5	64	32	6.61(54)	5.87(52)	7.67(64)

would allow one to better assess the effect on the spectrum and mixing angle of the axial anomaly, and connect this study to ongoing model-building and collider phenomenology programs. Furthermore, having demonstrated the viability of the numerical techniques, it would be interesting to understand how the results depend also on other intrinsic parameters of the theory, such as the numbers, $N_{\rm f}$ and $N_{\rm as}$, of fermions transforming on the fundamental and antisymmetric representation of the group. An interesting connection to more formal field-theory research topics would involve changing the group, within the $Sp(2N)$ class of theories, to explore the approach to the large-N limit. We plan to exploit all of these opportunities for further research in the future.

The supporting data for this paper are openly available from Ref. [199] and the analysis code from Ref [200].

ACKNOWLEDGMENTS

We would like to thank Giacomo Cacciapaglia, Gabriele Ferretti, Thomas Flacke, Anna Hasenfratz, Chulwoo Jung, and Sarada Rajeev, for useful discussions during the "PNU Workshop on Composite Higgs: Lattice study and all," at Haeundae, Busan, in February 2024, where preliminary results of this study were presented. The work of E. B. and B. L. is supported in part by the EPSRC ExCALIBUR programme ExaTEPP (Project No. EP/X017168/1). The work of E. B., B. L., M. P., and F. Z. has been supported by the STFC Consolidated Grant No. ST/X000648/1. The work of E. B. has also been supported by the UKRI Science and Technology Facilities Council (STFC) Research Software Engineering Fellowship No. EP/V052489/1. The work of N. F. has been supported by the STFC Doctoral Partnership Grant No. ST/X508834/1. The work of D. K. H. was supported by the Basic Science Research Program through the National Research Foundation of Korea (NRF) funded by the Ministry of Education (NRF-2017R1D1A1B06033701). The work of D. K. H. was further supported by the National Research Foundation of Korea (NRF) grant funded by the Korea government (MSIT) (2021R1A4A5031460). The work of J. W. L. is supported by IBS under the Project Code, No. IBS-R018-D1. The work of H. H. and C. J. D. L. is supported by the Taiwanese MoST Grant No. 109-2112-M-009-006-MY3 and NSTC Grant No. 112-2112-M-A49-021-MY3. The work of C. J. D. L. is also supported by Taiwanese National Science and Technology Council (NSTC) Grants No. 112-2639-M-002-006-ASP and No. 113-2119-M-007-013. The work of B. L. and M. P. has been further supported in part by the STFC Consolidated Grant No. ST/T000813/1. B. L. and M. P. received funding from the European Research Council (ERC) under the European Union's Horizon 2020 research and innovation program under Grant Agreement No. 813942. The work of D. V. is supported by STFC under Consolidated Grant No. ST/X000680/1. Numerical simulations have been performed on the DiRAC Extreme Scaling service at the University of Edinburgh, and on the DiRAC Data Intensive service at Leicester. The DiRAC Extreme Scaling service is operated by the Edinburgh Parallel Computing Centre on behalf of the STFC DiRAC HPC Facility (www.dirac.ac.uk). This equipment was funded by BEIS capital funding via STFC capital Grant No. ST/R00238X/1 and STFC DiRAC Operations Grant No. ST/R001006/1. DiRAC is part of the National e-Infrastructure.

APPENDIX: SYSTEMATIC EFFECTS RELATED TO THE CHOICE t_0

In principle, the value of t_0 in the GEVP should be chosen to be large in order to suppress systematic effects [188]. However, a choice of small t_0 can lead to smaller statistical uncertainties. In Table V we report the masses of the pseudoscalar singlet mesons as a function of t_0. We do not find any significant deviations.

TABLE V. The mass of the pseudoscalar singlet states as a function of t_0. When varying t_0 we find no deviations outside of statistical uncertainties.

Label	β	N_t	N_l	$am_0^{\rm f}$	$am_0^{\rm as}$	$am_{\eta'_h}(t_0=1)$	$am_{\eta'_h}(t_0=2)$	$am_{\eta'_h}(t_0=3)$	$am_{\eta'_h}(t_0=4)$	$am_{\eta'_h}(t_0=5)$
M1	6.5	48	20	−0.71	−1.01	0.6354(61)	0.6344(62)	0.6306(74)	0.6306(77)	0.634(10)
M2	6.5	64	20	−0.71	−1.01	0.621(13)	0.6239(74)	0.6225(92)	0.623(10)	0.623(11)
M3	6.5	96	20	−0.71	−1.01	0.592(13)	0.6111(76)	0.6079(92)	0.609(10)	0.620(18)
M4	6.5	64	20	−0.7	−1.01	0.6436(89)	0.6423(90)	0.643(11)	0.647(12)	0.658(13)
M5	6.5	64	32	−0.72	−1.01	0.667(26)	0.660(28)	0.668(21)	0.659(21)	0.651(20)

Label	β	N_t	N_l	$am_0^{\rm f}$	$am_0^{\rm as}$	$am_{\eta'_l}(t_0=1)$	$am_{\eta'_l}(t_0=2)$	$am_{\eta'_l}(t_0=3)$	$am_{\eta'_l}(t_0=4)$	$am_{\eta'_l}(t_0=5)$
M1	6.5	48	20	−0.71	−1.01	0.3769(96)	0.3968(34)	0.3900(43)	0.3836(68)	0.3913(69)
M2	6.5	64	20	−0.71	−1.01	0.3867(68)	0.3969(34)	0.3917(43)	0.3898(51)	0.3912(70)
M3	6.5	96	20	−0.71	−1.01	0.3826(67)	0.387634)	0.3826(41)	0.3815(48)	0.3750(84)
M4	6.5	64	20	−0.7	−1.01	0.4380(33)	0.4394(26)	0.4362(29)	0.4348(45)	0.4360(36)
M5	6.5	64	32	−0.72	−1.01	0.3590(53)	0.3582(54)	0.3617(33)	0.3586(63)	0.3615(36)

[1] A. Belyaev, G. Cacciapaglia, H. Cai, G. Ferretti, T. Flacke, A. Parolini, and H. Serodio, Di-boson signatures as standard candles for partial compositeness, J. High Energy Phys. 01 (2017) 094.

[2] D. B. Kaplan and H. Georgi, $SU(2) \times U(1)$ breaking by vacuum misalignment, Phys. Lett. **136B**, 183 (1984).

[3] H. Georgi and D. B. Kaplan, Composite Higgs and custodial SU(2), Phys. Lett. **145B**, 216 (1984).

[4] M. J. Dugan, H. Georgi, and D. B. Kaplan, Anatomy of a composite Higgs model, Nucl. Phys. **B254**, 299 (1985).

[5] D. B. Kaplan, Flavor at SSC energies: A New mechanism for dynamically generated fermion masses, Nucl. Phys. **B365**, 259 (1991).

[6] R. Barbieri, B. Bellazzini, V. S. Rychkov, and A. Varagnolo, The Higgs boson from an extended symmetry, Phys. Rev. D **76**, 115008 (2007).

[7] P. Lodone, Vector-like quarks in a "composite" Higgs model, J. High Energy Phys. 12 (2008) 029.

[8] B. Gripaios, A. Pomarol, F. Riva, and J. Serra, Beyond the minimal composite Higgs model, J. High Energy Phys. 04 (2009) 070.

[9] J. Mrazek, A. Pomarol, R. Rattazzi, M. Redi, J. Serra, and A. Wulzer, The other natural two Higgs doublet model, Nucl. Phys. **B853**, 1 (2011).

[10] D. Marzocca, M. Serone, and J. Shu, General composite Higgs models, J. High Energy Phys. 08 (2012) 013.

[11] C. Grojean, O. Matsedonskyi, and G. Panico, Light top partners and precision physics, J. High Energy Phys. 10 (2013) 160.

[12] J. Barnard, T. Gherghetta, and T. S. Ray, UV descriptions of composite Higgs models without elementary scalars, J. High Energy Phys. 02 (2014) 002.

[13] G. Cacciapaglia and F. Sannino, Fundamental composite (Goldstone) Higgs dynamics, J. High Energy Phys. 04 (2014) 111.

[14] G. Ferretti, UV completions of partial compositeness: The case for a SU(4) gauge group, J. High Energy Phys. 06 (2014) 142.

[15] A. Arbey, G. Cacciapaglia, H. Cai, A. Deandrea, S. Le Corre, and F. Sannino, Fundamental composite electroweak dynamics: Status at the LHC, Phys. Rev. D **95**, 015028 (2017).

[16] G. Cacciapaglia, H. Cai, A. Deandrea, T. Flacke, S. J. Lee, and A. Parolini, Composite scalars at the LHC: The Higgs, the sextet and the octet, J. High Energy Phys. 11 (2015) 201.

[17] G. von Gersdorff, E. Pontón, and R. Rosenfeld, The dynamical composite Higgs, J. High Energy Phys. 06 (2015) 119.

[18] F. Feruglio, B. Gavela, K. Kanshin, P. A. N. Machado, S. Rigolin, and S. Saa, The minimal linear sigma model for the Goldstone Higgs, J. High Energy Phys. 06 (2016) 038.

[19] T. DeGrand, M. Golterman, E. T. Neil, and Y. Shamir, One-loop chiral perturbation theory with two fermion representations, Phys. Rev. D **94**, 025020 (2016).

[20] S. Fichet, G. von Gersdorff, E. Pontón, and R. Rosenfeld, The excitation of the global symmetry-breaking vacuum in composite Higgs models, J. High Energy Phys. 09 (2016) 158.

[21] J. Galloway, A. L. Kagan, and A. Martin, A UV complete partially composite-pNGB Higgs, Phys. Rev. D **95**, 035038 (2017).

[22] A. Agugliaro, O. Antipin, D. Becciolini, S. De Curtis, and M. Redi, UV complete composite Higgs models, Phys. Rev. D **95**, 035019 (2017).

[23] N. Bizot, M. Frigerio, M. Knecht, and J.-L. Kneur, Nonperturbative analysis of the spectrum of meson resonances in an ultraviolet-complete composite-Higgs model, Phys. Rev. D **95**, 075006 (2017).

[24] C. Csaki, T. Ma, and J. Shu, Maximally symmetric composite Higgs models, Phys. Rev. Lett. **119**, 131803 (2017).

[25] M. Chala, G. Durieux, C. Grojean, L. de Lima, and O. Matsedonskyi, Minimally extended SILH, J. High Energy Phys. 06 (2017) 088.

[26] M. Golterman and Y. Shamir, Effective potential in ultraviolet completions for composite Higgs models, Phys. Rev. D **97**, 095005 (2018).

[27] J. Serra and R. Torre, Neutral naturalness from the brother-Higgs model, Phys. Rev. D **97**, 035017 (2018).

[28] C. Csáki, T. Ma, and J. Shu, Trigonometric parity for composite Higgs models, Phys. Rev. Lett. **121**, 231801 (2018).

[29] T. Alanne, D. Buarque Franzosi, and M. T. Frandsen, A partially composite Goldstone Higgs, Phys. Rev. D **96**, 095012 (2017).

[30] T. Alanne, D. Buarque Franzosi, M. T. Frandsen, M. L. A. Kristensen, A. Meroni, and M. Rosenlyst, Partially composite Higgs models: Phenomenology and RG analysis, J. High Energy Phys. 01 (2018) 051.

[31] F. Sannino, P. Stangl, D. M. Straub, and A. E. Thomsen, Flavor physics and flavor anomalies in minimal fundamental partial compositeness, Phys. Rev. D **97**, 115046 (2018).

[32] T. Alanne, N. Bizot, G. Cacciapaglia, and F. Sannino, Classification of NLO operators for composite Higgs models, Phys. Rev. D **97**, 075028 (2018).

[33] N. Bizot, G. Cacciapaglia, and T. Flacke, Common exotic decays of top partners, J. High Energy Phys. 06 (2018) 065.

[34] C. Cai, G. Cacciapaglia, and H.-H. Zhang, Vacuum alignment in a composite 2HDM, J. High Energy Phys. 01 (2019) 130.

[35] A. Agugliaro, G. Cacciapaglia, A. Deandrea, and S. De Curtis, Vacuum misalignment and pattern of scalar masses in the SU(5)/SO(5) composite Higgs model, J. High Energy Phys. 02 (2019) 089.

[36] G. Cacciapaglia, T. Ma, S. Vatani, and Y. Wu, Towards a fundamental safe theory of composite Higgs and dark matter, Eur. Phys. J. C **80**, 1088 (2020).

[37] H. Gertov, A. E. Nelson, A. Perko, and D. G. E. Walker, Lattice-friendly gauge completion of a composite Higgs with top partners, J. High Energy Phys. 02 (2019) 181.

[38] V. Ayyar, M. F. Golterman, D. C. Hackett, W. Jay, E. T. Neil, Y. Shamir *et al.*, Radiative contribution to the composite-Higgs potential in a two-representation lattice model, Phys. Rev. D **99**, 094504 (2019).

[39] G. Cacciapaglia, H. Cai, A. Deandrea, and A. Kushwaha, Composite Higgs and dark matter model in SU(6)/SO(6), J. High Energy Phys. 10 (2019) 035.
[40] D. Buarque Franzosi and G. Ferretti, Anomalous dimensions of potential top-partners, SciPost Phys. **7**, 027 (2019).
[41] G. Cacciapaglia, S. Vatani, and C. Zhang, Composite Higgs meets Planck scale: Partial compositeness from partial unification, Phys. Lett. B **815**, 136177 (2021).
[42] G. Cacciapaglia, A. Deandrea, T. Flacke, and A. M. Iyer, Gluon-photon signatures for color octet at the LHC (and beyond), J. High Energy Phys. 05 (2020) 027.
[43] Z.-Y. Dong, C.-S. Guan, T. Ma, J. Shu, and X. Xue, UV completed composite Higgs model with heavy composite partners, Phys. Rev. D **104**, 035013 (2021).
[44] G. Cacciapaglia, T. Flacke, M. Kunkel, and W. Porod, Phenomenology of unusual top partners in composite Higgs models, J. High Energy Phys. 02 (2022) 208.
[45] G. Ferretti, Compositeness above the electroweak scale and a proposed test at LHCb, EPJ Web Conf. **258**, 08002 (2022).
[46] A. Banerjee, D. B. Franzosi, and G. Ferretti, Modelling vector-like quarks in partial compositeness framework, J. High Energy Phys. 03 (2022) 200.
[47] H. Cai and G. Cacciapaglia, Partial compositeness under precision scrutiny, J. High Energy Phys. 12 (2022) 104.
[48] G. Cacciapaglia, A. Deandrea, M. Kunkel, and W. Porod, Coloured spin-1 states in composite Higgs models, J. High Energy Phys. 06 (2024) 092.
[49] R. Contino, Y. Nomura, and A. Pomarol, Higgs as a holographic pseudo-Goldstone boson, Nucl. Phys. **B671**, 148 (2003).
[50] K. Agashe, R. Contino, and A. Pomarol, The minimal composite Higgs model, Nucl. Phys. **B719**, 165 (2005).
[51] K. Agashe and R. Contino, The minimal composite Higgs model and electroweak precision tests, Nucl. Phys. **B742**, 59 (2006).
[52] K. Agashe, R. Contino, L. Da Rold, and A. Pomarol, A custodial symmetry for $Zb\bar{b}$, Phys. Lett. B **641**, 62 (2006).
[53] R. Contino, L. Da Rold, and A. Pomarol, Light custodians in natural composite Higgs models, Phys. Rev. D **75**, 055014 (2007).
[54] A. Falkowski and M. Perez-Victoria, Electroweak breaking on a soft wall, J. High Energy Phys. 12 (2008) 107.
[55] R. Contino, The Higgs as a composite Nambu-Goldstone boson, *Physics of the Large and the Small* (World Scientific, Singapore, 2011).
[56] R. Contino, D. Marzocca, D. Pappadopulo, and R. Rattazzi, On the effect of resonances in composite Higgs phenomenology, J. High Energy Phys. 10 (2011) 081.
[57] J. Erdmenger, N. Evans, W. Porod, and K. S. Rigatos, Gauge/gravity dynamics for composite Higgs models and the top mass, Phys. Rev. Lett. **126**, 071602 (2021).
[58] J. Erdmenger, N. Evans, W. Porod, and K. S. Rigatos, Gauge/gravity dual dynamics for the strongly coupled sector of composite Higgs models, J. High Energy Phys. 02 (2021) 058.
[59] D. Elander, M. Frigerio, M. Knecht, and J.-L. Kneur, Holographic models of composite Higgs in the Veneziano limit. Part I. Bosonic sector, J. High Energy Phys. 03 (2021) 182.
[60] D. Elander, M. Frigerio, M. Knecht, and J.-L. Kneur, Holographic models of composite Higgs in the Veneziano limit. Part II. Fermionic sector, J. High Energy Phys. 05 (2022) 066.
[61] J. Erdmenger, N. Evans, Y. Liu, and W. Porod, Holographic non-Abelian flavour symmetry breaking, Universe **9**, 289 (2023).
[62] D. Elander, A. Fatemiabhari, and M. Piai, Towards composite Higgs: Minimal coset from a regular bottom-up holographic model, Phys. Rev. D **107**, 115021 (2023).
[63] J. Erdmenger, N. Evans, Y. Liu, and W. Porod, Holography for $\mathrm{Sp}(2N_c)$ gauge dynamics: From composite Higgs to technicolour, J. High Energy Phys. 07 (2024) 169.
[64] D. Elander and M. Piai, Towards top-down holographic composite Higgs: Minimal coset from maximal supergravity, J. High Energy Phys. 03 (2022) 049.
[65] L. Vecchi, A dangerous irrelevant UV-completion of the composite Higgs, J. High Energy Phys. 02 (2017) 094.
[66] T. Appelquist, J. Ingoldby, and M. Piai, Nearly conformal composite Higgs model, Phys. Rev. Lett. **126**, 191804 (2021).
[67] T. Appelquist, J. Ingoldby, and M. Piai, Composite two-Higgs doublet model from dilaton effective field theory, Nucl. Phys. **B983**, 115930 (2022).
[68] T. Ma and G. Cacciapaglia, Fundamental composite 2HDM: SU(N) with 4 flavours, J. High Energy Phys. 03 (2016) 211.
[69] D. Buarque Franzosi, G. Cacciapaglia, and A. Deandrea, Sigma-assisted low scale composite Goldstone–Higgs, Eur. Phys. J. C **80**, 28 (2020).
[70] G. Panico and A. Wulzer, The composite Nambu-Goldstone Higgs, Lect. Notes Phys. **913**, 1 (2016).
[71] O. Witzel, Review on composite Higgs models, Proc. Sci. LATTICE2018 (**2019**) 006 [arXiv:1901.08216].
[72] G. Cacciapaglia, C. Pica, and F. Sannino, Fundamental composite dynamics: A review, Phys. Rep. **877**, 1 (2020).
[73] G. Ferretti and D. Karateev, Fermionic UV completions of composite Higgs models, J. High Energy Phys. 03 (2014) 077.
[74] G. Ferretti, Gauge theories of partial compositeness: Scenarios for Run-II of the LHC, J. High Energy Phys. 06 (2016) 107.
[75] G. Cacciapaglia, G. Ferretti, T. Flacke, and H. Serôdio, Light scalars in composite Higgs models, Front. Phys. **7**, 22 (2019).
[76] Y. Hochberg, E. Kuflik, T. Volansky, and J. G. Wacker, Mechanism for thermal relic dark matter of strongly interacting massive particles, Phys. Rev. Lett. **113**, 171301 (2014).
[77] Y. Hochberg, E. Kuflik, H. Murayama, T. Volansky, and J. G. Wacker, Model for thermal relic dark matter of strongly interacting massive particles, Phys. Rev. Lett. **115**, 021301 (2015).
[78] Y. Hochberg, E. Kuflik, and H. Murayama, SIMP spectroscopy, J. High Energy Phys. 05 (2016) 090.
[79] M. Hansen, K. Langæble, and F. Sannino, SIMP model at NNLO in chiral perturbation theory, Phys. Rev. D **92**, 075036 (2015).

[80] N. Bernal, X. Chu, and J. Pradler, Simply split strongly interacting massive particles, Phys. Rev. D **95**, 115023 (2017).

[81] A. Berlin, N. Blinov, S. Gori, P. Schuster, and N. Toro, Cosmology and accelerator tests of strongly interacting dark matter, Phys. Rev. D **97**, 055033 (2018).

[82] N. Bernal, X. Chu, S. Kulkarni, and J. Pradler, Self-interacting dark matter without prejudice, Phys. Rev. D **101**, 055044 (2020).

[83] V. Beylin, M. Y. Khlopov, V. Kuksa, and N. Volchanskiy, Hadronic and hadron-like physics of dark matter, Symmetry **11**, 587 (2019).

[84] Y.-D. Tsai, R. McGehee, and H. Murayama, Resonant self-interacting dark matter from dark QCD, Phys. Rev. Lett. **128**, 172001 (2022).

[85] D. Kondo, R. McGehee, T. Melia, and H. Murayama, Linear sigma dark matter, J. High Energy Phys. 09 (2022) 041.

[86] N. Bernal and X. Chu, $\mathbb{Z}_2$ SIMP dark matter, J. Cosmol. Astropart. Phys. 01 (2016) 006.

[87] J. Pomper and S. Kulkarni, Low energy effective theories of composite dark matter with real representations, arXiv:2402.04176.

[88] T. Appelquist, J. Ingoldby, and M. Piai, Dilaton forbidden dark matter, Phys. Rev. D **110**, 035013 (2024).

[89] I. Brivio, M. B. Gavela, L. Merlo, K. Mimasu, J. M. No, R. del Rey, and V. Sanz, ALPs effective field theory and collider signatures, Eur. Phys. J. C **77**, 572 (2017).

[90] B. Bellazzini, A. Mariotti, D. Redigolo, F. Sala, and J. Serra, *R*-axion at colliders, Phys. Rev. Lett. **119**, 141804 (2017).

[91] M. Bauer, M. Neubert, and A. Thamm, Collider probes of axion-like particles, J. High Energy Phys. 12 (2017) 044.

[92] H. Cai, T. Flacke, and M. Lespinasse, A composite scalar hint from di-boson resonances?, arXiv:1512.04508.

[93] A. Belyaev, G. Cacciapaglia, H. Cai, T. Flacke, A. Parolini, and H. Serôdio, Singlets in composite Higgs models in light of the LHC 750 GeV diphoton excess, Phys. Rev. D **94**, 015004 (2016).

[94] G. Cacciapaglia, G. Ferretti, T. Flacke, and H. Serodio, Revealing timid pseudo-scalars with taus at the LHC, Eur. Phys. J. C **78**, 724 (2018).

[95] A. Hietanen, R. Lewis, C. Pica, and F. Sannino, Fundamental composite Higgs dynamics on the lattice: SU(2) with two flavors, J. High Energy Phys. 07 (2014) 116.

[96] W. Detmold, M. McCullough, and A. Pochinsky, Dark nuclei. II. Nuclear spectroscopy in two-color QCD, Phys. Rev. D **90**, 114506 (2014).

[97] V. Drach, A. Hietanen, C. Pica, J. Rantaharju, and F. Sannino, Template composite dark matter: $SU(2)$ gauge theory with 2 fundamental flavours, Proc. Sci. LATTICE2015 (**2016**) 234 [arXiv:1511.04370].

[98] R. Arthur, V. Drach, M. Hansen, A. Hietanen, C. Pica, and F. Sannino, SU(2) gauge theory with two fundamental flavors: A minimal template for model building, Phys. Rev. D **94**, 094507 (2016).

[99] R. Arthur, V. Drach, A. Hietanen, C. Pica, and F. Sannino, $SU(2)$ gauge theory with two fundamental flavours: Scalar and pseudoscalar spectrum, arXiv:1607.06654.

[100] C. Pica, V. Drach, M. Hansen, and F. Sannino, Composite Higgs dynamics on the lattice, EPJ Web Conf. **137**, 10005 (2017).

[101] J.-W. Lee, B. Lucini, and M. Piai, Symmetry restoration at high-temperature in two-color and two-flavor lattice gauge theories, J. High Energy Phys. 04 (2017) 036.

[102] V. Drach, T. Janowski, C. Pica, J. Rantaharju, and F. Sannino, The scalar sector of $SU(2)$ gauge theory with $N_F = 2$ fundamental flavours, Proc. Sci. LATTICE2016 (**2017**) 229.

[103] V. Drach, T. Janowski, and C. Pica, Update on SU(2) gauge theory with NF $= 2$ fundamental flavours, EPJ Web Conf. **175**, 08020 (2018).

[104] V. Drach, T. Janowski, C. Pica, and S. Prelovsek, Scattering of Goldstone bosons and resonance production in a composite Higgs model on the lattice, J. High Energy Phys. 04 (2021) 117.

[105] V. Drach, P. Fritzsch, A. Rago, and F. Romero-López, Singlet channel scattering in a composite Higgs model on the lattice, Eur. Phys. J. C **82**, 47 (2022).

[106] L. S. Bowes, V. Drach, P. Fritzsch, A. Rago, and F. Romero-Lopez, 2-flavour $SU(2)$ gauge theory with exponential clover Wilson fermions, Proc. Sci. LATTICE2023 (**2024**) 094 [arXiv:2401.00589].

[107] E. Bennett, D. K. Hong, J.-W. Lee, C. J. D. Lin, B. Lucini, M. Piai, and D. Vadacchino, Sp(4) gauge theory on the lattice: Towards SU(4)/Sp(4) composite Higgs (and beyond), J. High Energy Phys. 03 (2018) 185.

[108] J.-W. Lee, E. Bennett, D. K. Hong, C. J. D. Lin, B. Lucini, M. Piai *et al.*, Progress in the lattice simulations of Sp($2N$) gauge theories, Proc. Sci. LATTICE2018 (**2018**) 192 [arXiv:1811.00276].

[109] E. Bennett, D. K. Hong, J.-W. Lee, C. J. D. Lin, B. Lucini, M. Piai, and D. Vadacchino, Sp(4) gauge theories on the lattice: $N_f = 2$ dynamical fundamental fermions, J. High Energy Phys. 12 (2019) 053.

[110] E. Bennett, D. K. Hong, J.-W. Lee, C.-J. D. Lin, B. Lucini, M. Mesiti, M. Piai, J. Rantaharju, and D. Vadacchino, $Sp(4)$ gauge theories on the lattice: Quenched fundamental and antisymmetric fermions, Phys. Rev. D **101**, 074516 (2020).

[111] B. Lucini, E. Bennett, J. Holligan, D. K. Hong, H. Hsiao, J.-W. Lee *et al.*, Sp(4) gauge theories and beyond the standard model physics, EPJ Web Conf. **258**, 08003 (2022).

[112] E. Bennett, J. Holligan, D. K. Hong, H. Hsiao, J.-W. Lee, C. J. D. Lin *et al.*, Progress in $Sp(2N)$ lattice gauge theories, Proc. Sci. LATTICE2021 (**2022**) 308 [arXiv:2111.14544].

[113] E. Bennett, D. K. Hong, H. Hsiao, J.-W. Lee, C. J. D. Lin, B. Lucini *et al.*, Lattice studies of the Sp(4) gauge theory with two fundamental and three antisymmetric Dirac fermions, Phys. Rev. D **106**, 014501 (2022).

[114] J.-W. Lee, E. Bennett, D. K. Hong, H. Hsiao, C. J. D. Lin, B. Lucini *et al.*, Composite dynamics in Sp(2N) gauge theories, EPJ Web Conf. **274**, 08005 (2022).

[115] E. Bennett, J. Holligan, D. K. Hong, H. Hsiao, J.-W. Lee, C. J. D. Lin, B. Lucini, M. Mesiti, M. Piai, and D. Vadacchino, Sp(2N) lattice gauge theories and extensions

of the standard model of particle physics, Universe **9**, 236 (2023).
[116] E. Bennett, H. Hsiao, J.-W. Lee, B. Lucini, A. Maas, M. Piai, and F. Zierler, Singlets in gauge theories with fundamental matter, Phys. Rev. D **109**, 034504 (2024).
[117] E. Bennett *et al.*, Symplectic lattice gauge theories in the Grid framework: Approaching the conformal window, Phys. Rev. D **108**, 094508 (2023).
[118] D. Mason, B. Lucini, M. Piai, E. Rinaldi, and D. Vadacchino, The deconfinement phase transition in $Sp(2N)$ gauge theories and the density of states method, Proc. Sci. LATTICE2023 (**2024**) 085. [arXiv:2310.02145].
[119] F. Zierler and A. Maas, $Sp(4)$ SIMP dark matter on the lattice, Proc. Sci. LHCP2021 (**2021**) 162.
[120] S. Kulkarni, A. Maas, S. Mee, M. Nikolic, J. Pradler, and F. Zierler, Low-energy effective description of dark $Sp(4)$ theories, SciPost Phys. **14**, 044 (2023).
[121] E. Bennett, D. K. Hong, H. Hsiao, J.-W. Lee, C. J. D. Lin, B. Lucini *et al.*, Lattice investigations of the chimera baryon spectrum in the Sp(4) gauge theory, Phys. Rev. D **109**, 094512 (2024).
[122] E. Bennett, J. Holligan, D. K. Hong, J.-W. Lee, C. J. D. Lin, B. Lucini *et al.*, On the spectrum of mesons in quenched $Sp(2N)$ gauge theories, Phys. Rev. D **109**, 094517 (2024).
[123] H. Hsiao, E. Bennett, D. K. Hong, J.-W. Lee, C. J. D. Lin, B. Lucini *et al.*, Chimera baryon spectrum in the Sp(4) completion of composite Higgs models, Proc. Sci. LATTICE2023 (**2024**) 089 [arXiv:2401.05637].
[124] G. Bergner and S. Piemonte, Lattice simulations of a gauge theory with mixed adjoint-fundamental matter, Phys. Rev. D **103**, 014503 (2021).
[125] G. Bergner and S. Piemonte, Mixed adjoint-fundamental matter and applications towards SQCD and beyond, Proc. Sci. LATTICE2021 (**2022**) 242 [arXiv:2111.15335].
[126] H. Hsiao, E. Bennett, D. K. Hong, J.-W. Lee, C. J. D. Lin, B. Lucini *et al.*, Spectroscopy of chimera baryons in a $Sp(4)$ lattice gauge theory, Proc. Sci. LATTICE2022 (**2022**) 211 [arXiv:2211.03955].
[127] V. Ayyar, T. DeGrand, M. Golterman, D. C. Hackett, W. I. Jay, E. T. Neil, Y. Shamir, and B. Svetitsky, Spectroscopy of SU(4) composite Higgs theory with two distinct fermion representations, Phys. Rev. D **97**, 074505 (2018).
[128] V. Ayyar, T. Degrand, D. C. Hackett, W. I. Jay, E. T. Neil, Y. Shamir, and B. Svetitsky, Baryon spectrum of SU(4) composite Higgs theory with two distinct fermion representations, Phys. Rev. D **97**, 114505 (2018).
[129] V. Ayyar, T. DeGrand, D. C. Hackett, W. I. Jay, E. T. Neil, Y. Shamir, and B. Svetitsky, Finite-temperature phase structure of SU(4) gauge theory with multiple fermion representations, Phys. Rev. D **97**, 114502 (2018).
[130] V. Ayyar, T. DeGrand, D. C. Hackett, W. I. Jay, E. T. Neil, Y. Shamir *et al.*, Partial compositeness and baryon matrix elements on the lattice, Phys. Rev. D **99**, 094502 (2019).
[131] G. Cossu, L. Del Debbio, M. Panero, and D. Preti, Strong dynamics with matter in multiple representations: SU(4) gauge theory with fundamental and sextet fermions, Eur. Phys. J. C **79**, 638 (2019).
[132] Y. Shamir, M. Golterman, W. I. Jay, E. T. Neil, and B. Svetitsky, S parameter from a prototype composite-Higgs model, Proc. Sci. LATTICE2021 (**2022**) 611 [arXiv:2110.05198].
[133] A. Lupo, M. Panero, N. Tantalo, and L. Del Debbio, Spectral reconstruction in SU(4) gauge theory with fermions in multiple representations, Proc. Sci. LATTICE2021 (**2022**) 092 [arXiv:2112.01158].
[134] L. Del Debbio, A. Lupo, M. Panero, and N. Tantalo, Multi-representation dynamics of SU(4) composite Higgs models: Chiral limit and spectral reconstructions, Eur. Phys. J. C **83** (2023) 220.
[135] A. Hasenfratz, E. T. Neil, Y. Shamir, B. Svetitsky, and O. Witzel, Infrared fixed point and anomalous dimensions in a composite Higgs model, Phys. Rev. D **107**, 114504 (2023).
[136] LatKMI Collaboration, Light composite scalar in eight-flavor QCD on the lattice, Phys. Rev. D **89**, 111502 (2014).
[137] T. Appelquist *et al.*, Strongly interacting dynamics and the search for new physics at the LHC, Phys. Rev. D **93**, 114514 (2016).
[138] LatKMI Collaboration, Light flavor-singlet scalars and walking signals in $N_f = 8$ QCD on the lattice, Phys. Rev. D **96**, 014508 (2017).
[139] A. D. Gasbarro and G. T. Fleming, Examining the low energy dynamics of walking gauge theory, Proc. Sci. LATTICE2016 (**2017**) 242 [arXiv:1702.00480].
[140] Lattice Strong Dynamics Collaboration, Nonperturbative investigations of SU(3) gauge theory with eight dynamical flavors, Phys. Rev. D **99**, 014509 (2019).
[141] LSD Collaboration, Hidden conformal symmetry from the lattice, Phys. Rev. D **108**, L091505 (2023).
[142] Lattice Strong Dynamics Collaboration, Light scalar meson and decay constant in SU(3) gauge theory with eight dynamical flavors, Phys. Rev. D **110**, 054501 (2024).
[143] Lattice Strong Dynamics Collaboration, Hidden conformal symmetry from eight flavors, Proc. Sci. LATTICE2023 (**2024**) 091 [arXiv:2401.00267].
[144] Z. Fodor, K. Holland, J. Kuti, D. Nogradi, C. Schroeder, and C. H. Wong, Can the nearly conformal sextet gauge model hide the Higgs impostor?, Phys. Lett. B **718**, 657 (2012).
[145] Z. Fodor, K. Holland, J. Kuti, S. Mondal, D. Nogradi, and C. H. Wong, Toward the minimal realization of a light composite Higgs, Proc. Sci. LATTICE2014 (**2015**) 244 [arXiv:1502.00028].
[146] Z. Fodor, K. Holland, J. Kuti, S. Mondal, D. Nogradi, and C. H. Wong, Status of a minimal composite Higgs theory, Proc. Sci. LATTICE2015 (**2016**) 219 [arXiv:1605.08750].
[147] Z. Fodor, K. Holland, J. Kuti, D. Nogradi, and C. H. Wong, The twelve-flavor β-function and dilaton tests of the sextet scalar, EPJ Web Conf. **175**, 08015 (2018).
[148] Z. Fodor, K. Holland, J. Kuti, and C. H. Wong, Tantalizing dilaton tests from a near-conformal EFT, Proc. Sci. LATTICE2018 (**2019**) 196 [arXiv:1901.06324].
[149] Z. Fodor, K. Holland, J. Kuti, and C. H. Wong, Dilaton EFT from p-regime to RMT in the ϵ-regime, Proc. Sci. LATTICE2019 (**2020**) 246 [arXiv:2002.05163].
[150] E. Bennett, L. D. Debbio, N. Forzano, R. Hill, D. K. Hong, H. Hsiao *et al.*, Meson spectroscopy from spectral densities in lattice gauge theories, arXiv:2405.01388.

[151] M. Hansen, A. Lupo, and N. Tantalo, Extraction of spectral densities from lattice correlators, Phys. Rev. D **99**, 094508 (2019).

[152] S. Gusken, U. Low, K. H. Mutter, R. Sommer, A. Patel, and K. Schilling, Nonsinglet axial vector couplings of the baryon octet in lattice QCD, Phys. Lett. B **227**, 266 (1989).

[153] S. Gusken, A study of smearing techniques for hadron correlation functions, Nucl. Phys. B, Proc. Suppl. **17**, 361 (1990).

[154] D. S. Roberts, W. Kamleh, D. B. Leinweber, M. S. Mahbub, and B. J. Menadue, Accessing high momentum states in lattice QCD, Phys. Rev. D **86**, 074504 (2012).

[155] C. Alexandrou, F. Jegerlehner, S. Gusken, K. Schilling, and R. Sommer, B meson properties from lattice QCD, Phys. Lett. B **256**, 60 (1991).

[156] APE Collaboration, Glueball masses and string tension in lattice QCD, Phys. Lett. B **192**, 163 (1987).

[157] M. Falcioni, M. L. Paciello, G. Parisi, and B. Taglienti, Again on SU(3) glueball mass, Nucl. Phys. **B251**, 624 (1985).

[158] D. A. Kosower, Symmetry-breaking patterns in pseudoreal and real gauge theories, Phys. Lett. **144B**, 215 (1984).

[159] J. B. Kogut, M. A. Stephanov, D. Toublan, J. J. M. Verbaarschot, and A. Zhitnitsky, QCD—like theories at finite baryon density, Nucl. Phys. **B582**, 477 (2000).

[160] E. Witten, Instantons, the quark model, and the 1/n expansion, Nucl. Phys. **B149**, 285 (1979).

[161] E. Witten, Current algebra theorems for the U(1) Goldstone boson, Nucl. Phys. **B156**, 269 (1979).

[162] G. Veneziano, U(1) without instantons, Nucl. Phys. **B159**, 213 (1979).

[163] N. H. Christ, C. Dawson, T. Izubuchi, C. Jung, Q. Liu, R. D. Mawhinney, C. T. Sachrajda, A. Soni, and R. Zhou, The η and η' mesons from lattice QCD, Phys. Rev. Lett. **105**, 241601 (2010).

[164] J. J. Dudek, R. G. Edwards, B. Joo, M. J. Peardon, D. G. Richards, and C. E. Thomas, Isoscalar meson spectroscopy from lattice QCD, Phys. Rev. D **83**, 111502 (2011).

[165] ETM Collaboration, η and η' mesons from $N_f = 2 + 1 + 1$ twisted mass lattice QCD, J. High Energy Phys. 11 (2012) 048.

[166] ETM Collaboration, η and η' mixing from lattice QCD, Phys. Rev. Lett. **111**, 181602 (2013).

[167] G. S. Bali, S. Collins, S. Dürr, and I. Kanamori, $D_s \to \eta, \eta'$ semileptonic decay form factors with disconnected quark loop contributions, Phys. Rev. D **91**, 014503 (2015).

[168] OTM Collaboration, A mixed action analysis of η and η' mesons, Nucl. Phys. **B896**, 470 (2015).

[169] ETM Collaboration, Flavor-singlet meson decay constants from $N_f = 2 + 1 + 1$ twisted mass lattice QCD, Phys. Rev. D **97**, 054508 (2018).

[170] RQCD Collaboration, Masses and decay constants of the η and η' mesons from lattice QCD, J. High Energy Phys. 08 (2021) 137.

[171] CSSM/QCDSF/UKQCD Collaborations, State mixing and masses of the $\pi 0$, η and η' mesons from $n_f = 1 + 1 + 1$ lattice QCD + QED, Phys. Rev. D **104**, 114514 (2021).

[172] RQCD Collaboration, Properties of the η and η' mesons: Masses, decay constants and gluonic matrix elements, Proc. Sci. LATTICE2021 (**2021**) 286 [arXiv:2111.05656].

[173] J. F. Simeth, Properties of the η and η' mesons from lattice QCD, Ph.D. thesis, Regensburg University, 2022.

[174] K. G. Wilson, Confinement of quarks, Phys. Rev. D **10**, 2445 (1974).

[175] P. Boyle, A. Yamaguchi, G. Cossu, and A. Portelli, Grid: A next generation data parallel C++ QCD library, arXiv:1512.03487.

[176] P. A. Boyle, G. Cossu, A. Yamaguchi, and A. Portelli, Grid: A next generation data parallel C++ QCD library, Proc. Sci. LATTICE2015 (**2016**) 023.

[177] A. Yamaguchi, P. Boyle, G. Cossu, G. Filaci, C. Lehner, and A. Portelli, Grid: OneCode and FourAPIs, Proc. Sci. LATTICE2021 (**2022**) 035 [arXiv:2203.06777].

[178] L. Del Debbio, A. Patella, and C. Pica, Higher representations on the lattice: Numerical simulations. SU(2) with adjoint fermions, Phys. Rev. D **81**, 094503 (2010).

[179] GitHub—CLAUDIOPICA/HiRep: HiRep repository—github.com, https://github.com/claudiopica/HiRep.

[180] GitHub—SA2C/HiRep: HiRep repository—github.com, https://github.com/sa2c/HiRep.

[181] GitHub—RJHudspith/GLU: GaugeLinkUtility repository—github.com, https://github.com/RJHudspith/GLU.

[182] M. Lüscher, Properties and uses of the Wilson flow in lattice QCD, J. High Energy Phys. 08 (2010) 071.

[183] M. Luscher and P. Weisz, Perturbative analysis of the gradient flow in non-Abelian gauge theories, J. High Energy Phys. 02 (2011) 051.

[184] M. Lüscher, Future applications of the Yang-Mills gradient flow in lattice QCD, Proc. Sci. LATTICE2013 (**2014**) 016 [arXiv:1308.5598].

[185] BMW Collaboration, High-precision scale setting in lattice QCD, J. High Energy Phys. 09 (2012) 010.

[186] C. Michael, Adjoint sources in lattice gauge theory, Nucl. Phys. **B259**, 58 (1985).

[187] M. Luscher and U. Wolff, How to calculate the elastic scattering matrix in two-dimensional quantum field theories by numerical simulation, Nucl. Phys. **B339** (1990) 222.

[188] B. Blossier, M. Della Morte, G. von Hippel, T. Mendes, and R. Sommer, On the generalized eigenvalue method for energies and matrix elements in lattice field theory, J. High Energy Phys. 04 (2009) 094.

[189] X. Jiang, W. Sun, F. Chen, Y. Chen, M. Gong, Z. Liu *et al.*, η-glueball mixing from $N_f = 2$ lattice QCD, Phys. Rev. D **107**, 094510 (2023).

[190] J. Foley, K. Jimmy Juge, A. O'Cais, M. Peardon, S. M. Ryan, and J.-I. Skullerud, Practical all-to-all propagators for lattice QCD, Comput. Phys. Commun. **172**, 145 (2005).

[191] S.-J. Dong and K.-F. Liu, Stochastic estimation with Z(2) noise, Phys. Lett. B **328**, 130 (1994).

[192] S. Aoki, H. Fukaya, S. Hashimoto, and T. Onogi, Finite volume QCD at fixed topological charge, Phys. Rev. D **76**, 054508 (2007).

[193] T. Umeda, A constant contribution in meson correlators at finite temperature, Phys. Rev. D **75**, 094502 (2007).

[194] HPQCD Collaboration, Constrained curve fitting, Nucl. Phys. B, Proc. Suppl. **106**, 12 (2002).

[195] P. Lepage, GPLEPAGE/CORRFITTER: CORRFITTER version 8.2, 10.5281/zenodo.5733391 (2021).

[196] R. Kaiser and H. Leutwyler, Pseudoscalar decay constants at large N_c, in *Workshop on Methods of Nonperturbative Quantum Field Theory* (World Scientific, Singapore, 1998), pp. 15–29.

[197] T. Feldmann, P. Kroll, and B. Stech, Mixing and decay constants of pseudoscalar mesons, Phys. Rev. D **58**, 114006 (1998).

[198] W. Wilcox, Noise methods for flavor singlet quantities, in *Interdisciplinary Workshop on Numerical Challenges in Lattice QCD* (1999), pp. 127–141, arXiv:hep-lat/9911013.

[199] E. Bennett, N. Forzano, D. K. Hong, H. Hsiao, J.-W. Lee, C.-J. D. Lin *et al.*, On the mixing between flavor singlets in lattice gauge theories coupled to matter fields in multiple representations—data release, 10.5281/zenodo.13349269 (2024).

[200] E. Bennett, N. Forzano, D. K. Hong, H. Hsiao, J.-W. Lee, C.-J. D. Lin *et al.*, On the mixing between flavor singlets in lattice gauge theories coupled to matter fields in multiple representations—workflow release, 10.5281/zenodo.13349298 (2024).